

Synthetic example

The shots, considered the observed data, were generated by propagating the wavelet in blue in Figure 2 through the velocity model (Figure 3A) by applying constant-density acoustic finite-difference modelling. The initial model for the inversion (Figure 3B) was constructed by applying a Gaussian smoother to the true model. An example of an observed shot located at the middle of the model is shown in Figure 3C. The initial frequency range was from 1 to 6 Hz, and then it was moved up by 1 Hz in each iteration. The calibration well C is located at the middle of the model; its top and base are 400 and 900 m, respectively.

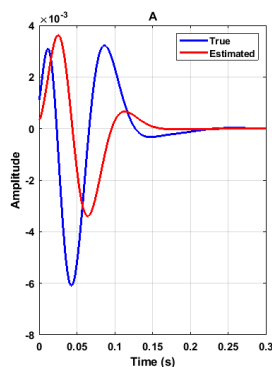


Fig.2. True and initial wavelet.

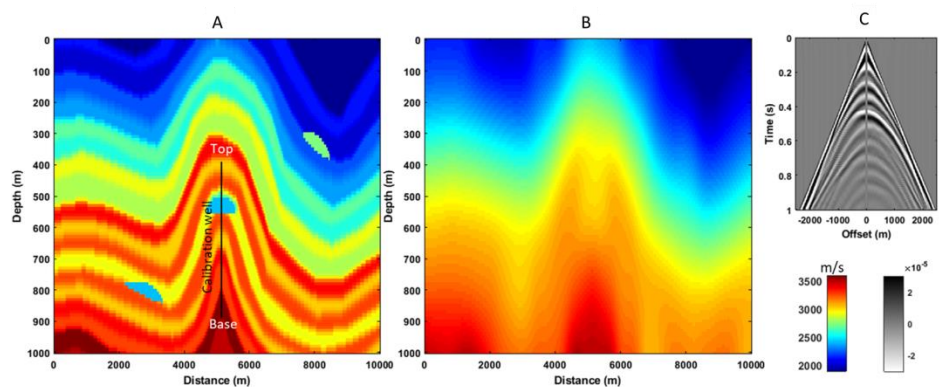


Fig. 3. A) True model and calibration well. B) Initial model. C) Observed shot.

We applied the methodology to update the amplitude and phase of the modelled data using the initial wavelet in red in Figure 2. This wavelet was estimated from the seismic. The inversion result is shown in Figure 4. We are able to recover the true model diminishing most of the negative effects that the wrong wavelet produces. The errors tend to decrease after iteration 10 when the wavelet has been already corrected as shown in Figure 5.

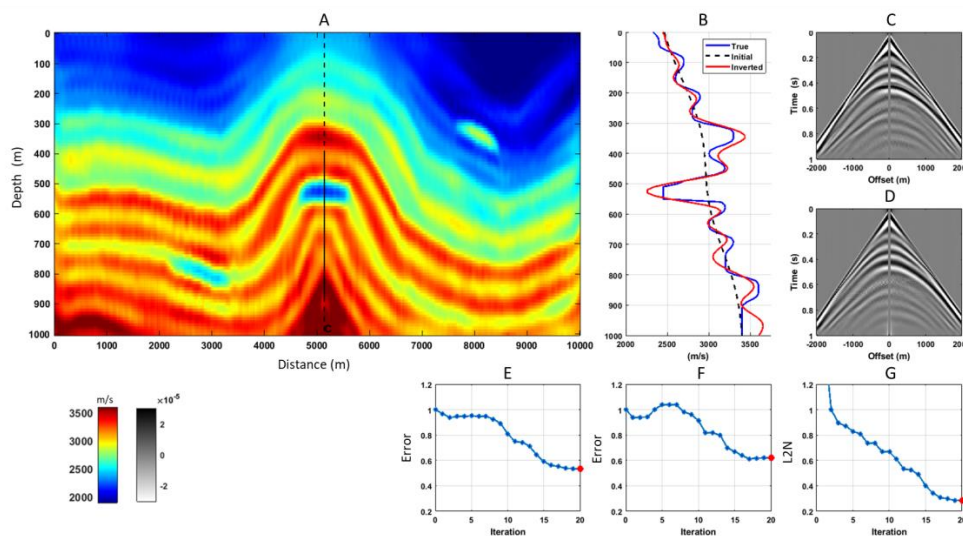


Fig. 4. A) Inverted model with the wrong initial wavelet estimated from the seismic data and applying the process of phase and amplitude updating. B) Inverted velocity in calibration well. C) Observed shot. D) Modelled shot. E) Error in inverted model. F) Error in calibration well. G) L2N of the data residuals.

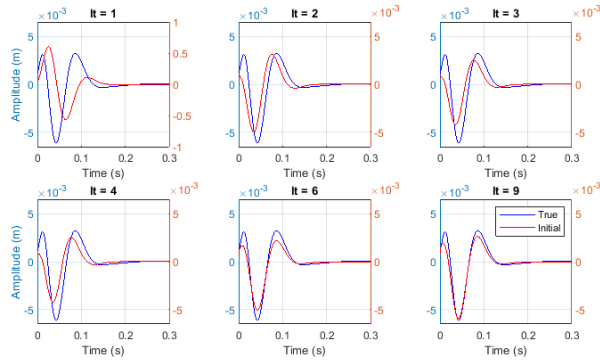


FIG. 5. Evolution of the wavelet for selected iterations. The wavelet has been practically recovered after iteration 10.

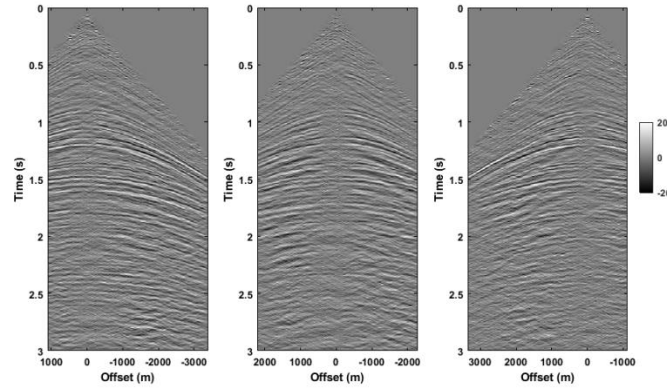


FIG. 6. Hussar's shots used for the inversion. Evolution of the wavelet for selected iterations.

Application on Hussar dataset

Figure 6 shows the shots used for the inversion (Isaac and Margrave, 2011). Radial filtering, Gabor deconvolution, low-pass and FK filtering were applied. Figure 7 shows the inversion result for Hussar dataset. At the zone, where we have significant seismic events from 0.8 seconds (approximately 1000 m of depth), the inverted velocity shows a reasonable agreement with the velocity measure in the wells. However, in the shallow zone where the lack of seismic information is evident, the velocity is not effectively recovered.

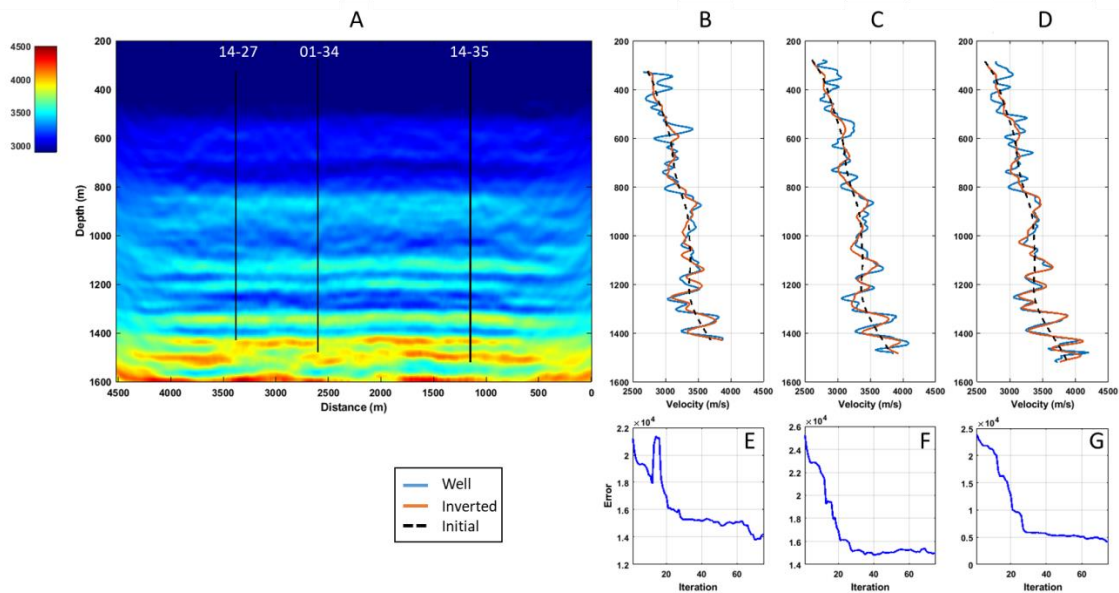


FIG. 7. A) Inverted model for Hussar dataset. B) Inverted velocity in well 14-27. C) Inverted velocity in well 01-34. D) Inverted velocity in calibration well 14-35. E) Error in inverted velocity for well 14-27. F) Error in inverted velocity for well 01-34. G) Error in inverted velocity for calibration well 14-35.

In the synthetic example we saw that the amplitude-and-phase wavelet updates don't have significant changes after the 10 iterations, showing stability in the process. This is not happening for the case of Hussar dataset as it's shown in 8, where the evolution of the wavelet with iterations is displayed. The latter suggests that the process of updating the modelled reflectivity

before constructing the gradient has the greatest weight in the process. This methodology seems to be robust enough to be applied on real data.

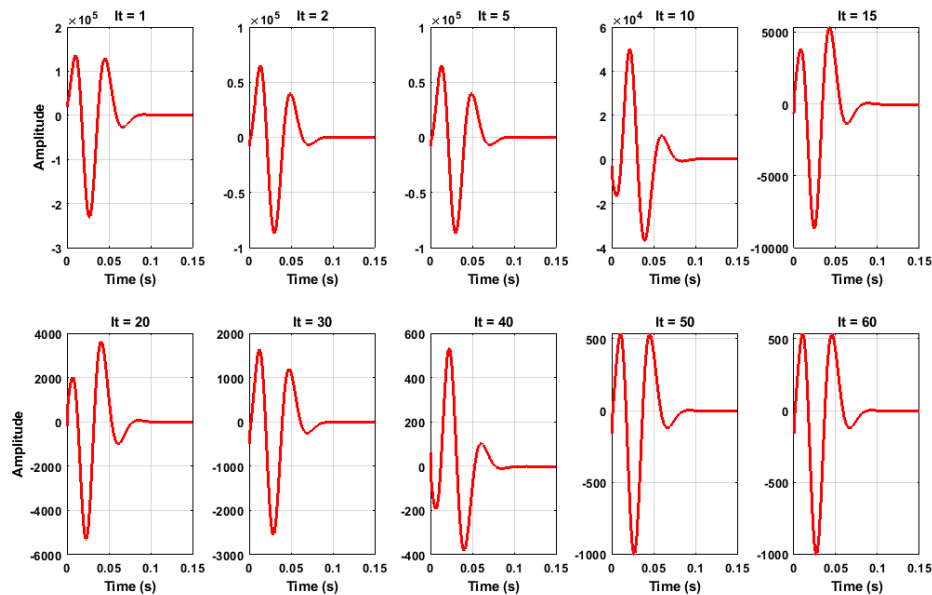


Fig. 8. Evolution of the wavelet for Hussar's inversion.

Conclusions

We proposed a methodology to diminish the negative impact that a wrong initial wavelet produces in the FWI process. Our methodology consists in separating the migration of the observed and modelled data previous to the construction of the gradient. Experiments with synthetic data show that the scheme is stable. We applied the process to the Hussar dataset, obtaining encouraging results. However, the high variability of the wavelet for the case of real data brings certain questions about the validity of the updated wavelet and suggests that the inversion relies on the matching process of the observed and modelled reflectivity datasets. In future work, we will address the issue of the instability of the updated wavelet that we saw in the real seismic data.

Acknowledgements

We thank the sponsors of CREWES. We acknowledge support from NSERC through the grant CRDPJ 461179-13. Author 1 thanks PEMEX and the government of Mexico for founding this research.

References

- Arenrin, B., and Margrave, G. F., 2015, Full waveform inversion of Hussar synthetics: CREWES Research Report, 27.
- Guarido, M., Lines, L., and Ferguson, R., 2014, Full waveform inversion - a synthetic test using the PSPI migration: CREWES Research Report, 26.
- Henley, D. C., 1999, Coherent noise attenuation in the radial trace domain: Introduction and demonstration: CREWES Research Report, 11.

- Isaac, J. H., and Margrave, G. F., 2011, Hurrah for hussar! Comparisons of stacked data: CREWES Research Report, 23.
- Lailly, P., 1983, The seismic inverse problem as a sequence of before stack migration: SIAM, 206–220.
- Lee, K. H., and Kim, H. J., 2003, Source-independent full-waveform inversion of seismic data: Geophysics, 68, No. 6, 2010–2015.
- Liu, S., Meng, X., and Fu, L., 2016, Source wavelet independent time-domain full waveform inversion (FWI) of cross-hole radar data, in Geoscience and Remote Sensing Symposium (IGARSS), 2016 IEEE International, IEEE, 7485–7488.
- Margrave, G. F., 2014, Post-stack iterative modeling migration and inversion (IMMI): CREWES Research Report, 27.
- Margrave, G. F., Bertram, M. B., Lawton, D. C., Innanen, K. A., Hall, K. W., Mewhort, L., and Hall, M., 2011a, The Hussar low-frequency experiment: CREWES Research Report, 23.
- Margrave, G. F., Ferguson, R. J., and Hogan, C. M., 2010, Full waveform inversion with wave equation migration and well control: CREWES Research Report, 22.
- Margrave, G. F., Lamoureux, M. P., and Henley, D. C., 2011b, Gabor deconvolution: Estimating reflectivity by nonstationary deconvolution of seismic data: Geophysics, 76, No. 3, W15–W30.
- Pan, W., Margrave, G., and Innanen, K. A., 2013, On the role of the deconvolution imaging condition in full waveform inversion: CREWES Research Report, 25.
- Pan, W., Margrave, G. F., and Innanen, K. A., 2014, Iterative modeling migration and inversion (IMMI): Combining full waveform inversion with standard inversion methodology: 84th Ann. Internat. Mtg., SEG, Expanded Abstracts, 938–943.
- Romahn, S., and Innanen, K. A., 2017, Iterative modeling, migration, and inversion: Evaluating the well calibration technique to scale the gradient in the full waveform inversion process: SEG Technical Program Expanded Abstracts 2017, 1583–1587.
- Romahn, S., and Innanen, K. A., 2018, FWI with wave equation migration: well validation vs data validation vs well-and-data validation: CREWES Research Report, 30.
- Tarantola, A., 1984, Inversion of seismic reflection data in the acoustic approximation: Geophysics, 49, 1259–1266.